# Galactoxylomannans from *Cryptococcus neoformans* Varieties *neoformans* and *grubii* Are Structurally and Antigenically Variable[▽]

Magdia De Jesus,[1]† Siu-Kei Chow,[1]† Radames J. B. Cordero,[1]
Susana Frases,[1] and Arturo Casadevall[1,2]*

*Department of Microbiology and Immunology[1] and Division of Infectious Diseases of the Department of
Medicine,[2] Albert Einstein College of Medicine, 1300 Morris Park Avenue, Bronx, New York 10461*

Prior studies have established that the *Cryptococcus neoformans* capsular polysaccharide component galactoxylomannan (GalXM) manifests serotype-related structural differences that translate into antigenic differences. We analyzed GalXM from acapsular serotype A and D strains by carbohydrate analysis and static and dynamic light scattering to determine mass, effective diameter, polydispersity, and diffusion coefficients. Multiangle laser light scattering showed that GalXM from *C. neoformans* var. *grubii* strain cap59 (serotype A) had larger molecular mass ($4.21 \times 10^6 \pm 0.95 \times 10^6$ g/mol) and radius of gyration ($207 \pm 27$ nm) than GalXM from *C. neoformans* var. *neoformans* cap67 (serotype D). cap67 GalXM had corresponding values of $0.70 \times 10^6 \pm 0.05 \times 10^6$ g/mol and $120 \pm 22$ nm, respectively. The effective diameter for GalXM and polydispersity from the two strains varied depending on temperature and medium growth conditions, indicating that GalXM structure can vary within a strain, depending on its environment. Zeta potential determinations were negative for GalXM from both strains under all conditions, consistent with the recently reported presence of glucuronic acid. These results imply that *C. neoformans* GalXM, like glucuronoxylomannan, can manifest variety- and growth condition-related variations. Analysis of 16 *C. neoformans* and 7 *Cryptococcus gattii* strains with polyclonal antibody to a GalXM strain revealed antigenic similarities among the *C. neoformans* variety *neoformans* and *grubii* strains and no reactivity with *C. gattii*. As a result of the deleterious effects of GalXM on immune function, structural and antigenic variability between serotypes may translate into differences in immunomodulatory effects.

The encapsulated fungal pathogen *Cryptococcus neoformans* causes disease primarily in individuals with impaired immunity (22). Cryptococcosis is relatively common in individuals with late-stage human immunodeficiency virus or certain cancers and in organ transplant recipients (22, 25, 31). *C. neoformans* has several well-defined virulence factors that include a polysaccharide (PS) capsule (23, 31). The capsular polysaccharide was classically defined as being composed of glucuronoxylomannan (GXM), galactoxylomannan (GalXM), and mannoproteins (MP) (19, 24, 29). However, this composition was inferred based on analysis of culture-shed exopolysaccharide (6, 18). Recent studies suggest that the capsule is made of GXM while GalXM and mannoproteins appear to be primarily export products (10, 17).

GXM has been extensively studied, but considerably less is known about GalXM (5, 6). Earlier structural studies of GalXM revealed that GalXM constitutes about 8% of the shed polysaccharide found in cryptococcal culture supernatants (1, 29) and has an α-1,6-galactan backbone containing four potential short oligosaccharide branch structures. The branches are 3-O-linked to the backbone and consist of an α-1,3-mannose,

α-1,4-mannose, and β-galactosidase trisaccharide with variable amounts of β-1,2- or β-1,3-xylose side groups (1, 21, 29). The GalXM backbone consists of galactopyranose and a small amount of galactofuranose (29), unlike GXM, which contains only mannopyranose (1). Recently, it was found that the residue that is ($1{\rightarrow}3$)-linked to the side chain galactose of GalXM is β-D-glucuronic acid, instead of β-D-xylose as previously determined. It was proposed that the GalXM polymer be renamed to "glucuronoxylomannogalactan" (GXMGal) due to the presence of glucuronic acid (16). Heiss et al. suggest that the nomenclature accurately represents both the polymer composition and structure (16). Although we agree that GXMGal is a better term for this polysaccharide based on the existing information, we will continue to use GalXM for now to maintain the continuity of the literature. It is conceivable that as structural knowledge accumulates, additional revisions to the nomenclature will be needed in the future. The latter concern is heightened by data presented in the manuscript showing considerable variability in GalXM structure under different conditions. Several recent studies indicate that GalXM is a potent immunomodulator with pleiotropic deleterious effects on the immune system (2, 9, 26, 30).

Studies with GalXM from cap67 revealed an average mass of $1 \times 10^5$ Da (1, 21), which was significantly smaller than that of GXM ($1.7 \times 10^6$ Da) (21). Since GalXM has a smaller molecular mass, GalXM is the most numerous component among shed capsular polysaccharide fractions on a molar basis,

* Corresponding author. Mailing address: Department of Microbiology and Immunology, Albert Einstein College of Medicine, 1300 Morris Park Ave., Bronx, NY 10461. Phone: (718) 430-2215. Fax: (718) 430-8968. E-mail: arturo.casadevall@einstein.yu.edu.
† M.D.J. and S.-K.C. contributed equally to this work.
▽ Published ahead of print on 8 January 2010.

TABLE 1. Glycosyl composition analysis

| Strain and component | Composition under the indicated condition (mol%)[a] | | | | | | | |
|---|---|---|---|---|---|---|---|---|
| | Temp | | | | Medium[b] | | | |
| | 25°C | 30°C | 37°C | 40°C | Minimal | Sab | YPD | Pep-Gal |
| cap67 | | | | | | | | |
| Xyl | 10.8 | 14.1 | 5.0 | 14.5 | NA | 13.8 | 15.8 | 13.0 |
| GlcA | 1.2 | 2.0 | 2.3 | 3.3 | NA | | | |
| GalA | | | | | NA | | | |
| Man | 38.9 | 33.5 | 51.3 | 30.9 | NA | 24.5 | 27.7 | 24.8 |
| Gal | 44.8 | 48.9 | 35.2 | 50.1 | NA | 56.8 | 49.5 | 57.7 |
| Glc | 3.7 | 1.0 | 3.9 | 1.0 | NA | 4.8 | 7.0 | 4.4 |
| cap59 | | | | | | | | |
| Xyl | 6.1 | 7.2 | 10.7 | 9.2 | 15.8 | 13.9 | 13.3 | 10.5 |
| GlcA | | 3.3 | 3.1 | 3.1 | 1.9 | | | |
| GalA | | | | | | | | |
| Man | 37.5 | 28.9 | 31.0 | 32.3 | 25.8 | 25.6 | 31.0 | 16.1 |
| Gal | 52.6 | 58.8 | 53.8 | 54.2 | 54.2 | 58.7 | 53.0 | 69.5 |
| Glc | 3.7 | 1.1 | 1.3 | 1.3 | 2.3 | 1.8 | 2.7 | 3.8 |

[a] NA, data were not available due to low sample recovery.
[b] Sab, Sabouraud's broth; Pep-Gal, peptone supplemented with galactose.

with 2 to 3.5 mol of GalXM for each mole of GXM (21). Recently, we showed that GalXM is primarily an exopolysaccharide and that there are serotype-related structural differences in GalXM, based on nuclear magnetic resonance (NMR) analysis, that could translate into antigenic variability (10). Here, we follow up on that lead using carbohydrate analysis, light scattering, and zeta potential measurements to show that there are strain- and serotype-related differences in GalXM structure that could be enhanced by growth conditions.

(The data in this paper are from a thesis submitted by M. De Jesus (Ph.D. awarded in June 2009) and S.-K. Chow in partial fulfillment of the requirements for a Ph.D. from the Albert Einstein College of Medicine, Yeshiva University, Bronx, NY.)

## MATERIALS AND METHODS

***C. neoformans* strains.** *C. neoformans* var. *grubii* acapsular mutant cap59 was derived from strain H99 (MATα and hygromycin resistant; serotype A) and was a kind gift of Joseph Heitman at Duke University. *C. neoformans* var. *neoformans* acapsular mutant cap67 was derived from strain B3501 (serotype D) and was obtained from the American Type Culture Collection (Manassas, VA). cap67 is also known in the literature as B-4131, and its capsular phenotype in this strain can be restored by the CAP59 gene (3). Hence, cap59 and cap67 are derived from serotype A and D strains that are both complemented with the same gene, which appears to function in capsular polysaccharide export (15). In the immunofluorescence studies, eight *C. neoformans* var. *grubii* (serotype A), eight *C. neoformans* var. *neoformans* (serotype D), and seven *C. gattii* (serotype B and C) strains were used. H99 (serotype A) was obtained from the New York State Herbarium, Albany, NY, and the rest of the serotype A isolates were obtained from cryptococcal meningitis patients from New York City hospitals (28). Strains 24067, B3501, and Jec21 and five other clinical isolates were used in the serotype D group. The *C. gattii* strains included NIH isolates 18, 34, 112, 191, 444, 1343, and 3939. These isolates have been described previously (4).

**GalXM isolation.** GalXM was isolated as previously described (10). Briefly, a 400-ml culture of a *C. neoformans* acapsular mutant of strain cap67 or cap59 was grown under one of the following conditions: peptone medium supplemented with 2% galactose, minimal medium (15 mM glucose, 10 mM MgSO₄, 29.4 mM KH₂PO₄, 13 mM glycine, and 3 μM thiamine-HCl; pH 5.5), yeast extract-peptone-dextrose (YPD; Difco Laboratories, Detroit, MI), or Sabouraud's dextrose broth (Difco Laboratories, Detroit, MI) for 7 days. For the experiments to evaluate the effect of temperature, *C. neoformans* was grown in peptone supplemented with 2% galactose at 25, 30, 37, or 40°C for 7 days. The culture supernatant was separated from the cells by centrifugation at 900 × g for 15 min at room temperature and then concentrated using an Amicon centrifugal filter with

a 10,000-molecular-weight (MW) cutoff (Millipore, Bedford, MA). The material was then dialyzed for 1 week against distilled water, and the 10-kDa retentate, containing GalXM and mannoproteins, was passed through a 0.2-μm-pore-size filter. The resulting filtrate was then lyophilized and stored at room temperature. The freeze-dried mixture was dissolved in 25 ml of start buffer [0.01 M Tris base and 0.5 M NaCl solution, pH 7.2, to which CaCl₂ and Mn(II)Cl₂ was sequentially added to final concentrations of 1 mM]. To separate the GalXM and mannoproteins, the solution was then continuously passed through a concanavalin A-Sepharose 4B column (2.5 by 10 cm) (Sigma) for 16 h at 4°C using a peristaltic pump with a flow rate of 16 ml/h. The flowthrough as well as five column washes with start buffer were collected as 25-ml fractions (21). To identify carbohydrate-containing fractions, we tested these using a phenol-sulfuric acid assay (11). The fractions were combined, concentrated by ultrafiltration, and dialyzed against water for 3 days. GalXM was then recovered by lyophilization.

**GalXM glycosyl composition analysis.** GalXM samples were dissolved in methanol–1 M HCl and incubated at 80°C for 18 h. Methanolyzed samples were then per-*O*-trimethylsilylated by treatment with Tri-Sil (Pierce) for 30 min at 80°C. The per-*O*-trimethylsilyl (TMS) derivatives were analyzed by gas chromatography coupled to mass spectrometry (GC-MS). The derivatized structures were first separated on an HP 5890 gas chromatograph using a Supelco DB-1 fused silica capillary column (30 m by 0.25-mm internal diameter). Peaks detected by GC were fragmented in a 5970 MSD mass spectrometer, interfaced to the gas chromatograph. Carbohydrate standards included arabinose, rhamnose, fucose, xylose, glucuronic acid, galacturonic acid, mannose, galactose, glucose, mannitol, dulcitol, and sorbitol.

**Molecular mass determination.** Molecular masses were determined and calculated by multiangle laser light scattering as described by McFadden et al. and Frases et al. (12, 13, 21).

**Zeta potential measurements.** Zeta potential (ζ), particle mobility, and shift frequency of polysaccharide samples were calculated in a zeta potential analyzer (ZetaPlus; Brookhaven Instruments Corp., Holtsville, NY). Zeta is a measurement of charge (in millivolts) defined as the potential gradient that develops across the interface between a boundary liquid in contact with a solid and the

TABLE 2. GalXM molecular properties calculated by multiangle laser light scattering in a molecular weight analyzer

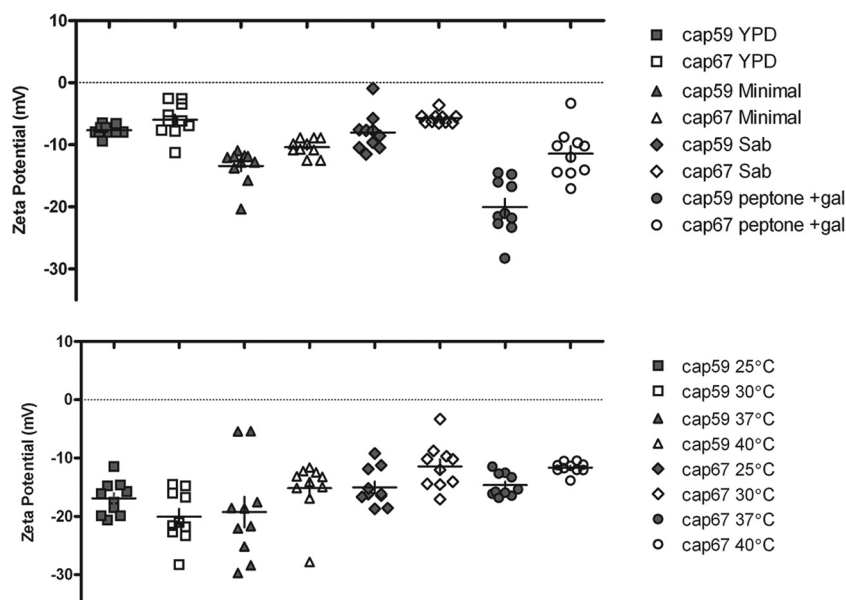| GalXM source | Refractive index (dn/dc at 620 nm) | $M_w$ ($10^6$ [g/mol]) | Rg (nm) | $M_w$/Rg ($10^3$)[a] | $A_2$ ($10^{-3}$ [cm³ mol/2]) |
|---|---|---|---|---|---|
| cap59 | 0.1923 | 4.21 ± 0.95 | 207 ± 27 | 20.34 | 0.26 ± 0.12 |
| cap67 | 0.1982 | 0.70 ± 0.05 | 120 ± 22 | 5.83 | −4.20 ± 3.60 |

[a] Mass density.

FIG. 1. Growth temperature and medium dependence of zeta potential measurements. (Top) Zeta potential measurements in mV for GalXM from strains cap59 and cap67 grown in different media: YPD medium, minimal medium, Sabouraud's dextrose broth (Sab), and peptone medium supplemented with 2% galactose. (Bottom) Zeta potential measurements in mV for strains cap59 and cap67 grown at different temperatures.

mobile diffuse layer in the body of the liquid. Derivation of zeta potential is described in Frases et al. (12).

**GalXM particle sizes.** The effective diameter and the polydispersity of GalXM preparations were measured by quasi-electric light scattering (QELS) or multiangle laser light scattering in a 90Plus/BI-MAS Multi-Angle Particle Sizing analyzer (Brookhaven Instruments Corp., Holtsville, NY). The protocol used to measure particle size is described in Frases et al. (12, 13). Both GalXM samples were analyzed under the same conditions.

**Immunofluorescence.** Sixteen *C. neoformans* strains (eight each of serotypes A and D, respectively) and seven *C. gattii* strains (three of serotype B and four of serotype C) were grown in Sabouraud dextrose broth (Difco Laboratories, Detroit, MI) for 1 day at 30°C. The cells were then transferred to capsule-inducing medium (1:10 Sabouraud broth-morpholinepropanesulfonic acid [MOPS], 50 mM, pH 7.3) for another day of incubation at 30°C. In the experiment associated with the growth curve study, the strains were grown in 1:1 Sabouraud broth–50 mM MOPS, pH 7.3, to optimize cell growth and capsule induction. The cells were washed three times with phosphate-buffered saline (PBS; pH 7.4) and counted with a hemocytometer. For GalXM staining using GalXM-PA (where PA is protective antigen) polyclonal serum (10), $2 \times 10^6$ cells in 100 µl of immunofluorescence buffer (1% bovine serum albumin [BSA] and 0.05% goat serum in PBS) were incubated with 4 µl of serum for 1 h at room temperature. Cells were washed three times with buffer and incubated with a 1:25 dilution of goat anti-rat IgM-fluorescein isothiocyanate (FITC) as the secondary antibody for 1 h at room temperature. Cells were then washed and incubated with 1:10,000 Uvitex 2B (Polysciences Inc.) in PBS for 20 min. Stained cells were suspended in mounting medium (50% glycerol and 50 mM *N*-propyl gallate in PBS) and imaged by epifluorescence microscopy on a Zeiss Axioskop 200 inverted microscope equipped with a cool charge-coupled device using a 63×, 1.4-numerical aperture (NA) objective with a 1.6× optovar. Images were acquired using the same exposure times and microscopic settings and processed by Axio Vision, version 4.6, software (Carl Zeiss Micro Imaging, New York, NY).

**Quantification of GalXM labeling.** Fifteen randomly selected fields of view were imaged for each strain. The cells were stained with Uvitex 2B, and the images were focused on the plane of the cell wall to avoid bias in locating GalXM staining. The total number of cells and the number of GalXM-labeled cells in the field of view were recorded digitally and counted, and the percentage of labeled cells was calculated in each strain. To study the GalXM staining pattern with polyclonal antibody, the number of discrete fluorescent signals on the capsule (expressed in dots) was counted on each labeled cell and categorized into four groups (1 to 5, 6 to 10, 11 to 15, and >15 dots) (see Fig. 7). This method did not count all the fluorescent signals on the labeled cell but was limited to those signals on the equatorial plane defined by focusing the microscope on the cell

wall. In the experiment associated with the growth curve study, optical density was read at 620 nm for 2.5 days with six time points (0, 12, 24, 36, 48, and 60 h). At each interval except 0 h, cells were stained as described above and imaged using the same microscope setting. Thirty randomly selected fields of view were imaged followed by GalXM staining quantification.

**Statistical analysis.** Statistical and computation analyses of light scattering measurements were carried out with Bi-ZPMwA Zimm Plot software (Brookhaven Instruments Corp., Holtsville, NY) to calculate $M_w$, radius of gyration (Rg) and the second virial coefficient ($A_2$). The software 90Plus/BI-MAS was used for effective diameter, polydispersity, and diffusion coefficient parameters (Brookhaven Instruments Corp., Holtsville, NY). For each sample we isolated two different preparations of GalXM per condition. We then examined each polysaccharide preparation per condition and took 10 measurements for each sample. Error was calculated from 10 measurements of one sample. Zeta Plus software was used for zeta potential, mobility, and frequency shift data (Brookhaven Instruments Corp., Holtsville, NY). Student's *t* test was used in the immunofluorescence study comparing serotypes A and D.

## RESULTS

**Glycosyl composition.** GalXM samples were subjected to acidic methanolysis, and their monosaccharide constituents were analyzed by gas chromatography. This analysis allows the potential detection of four different forms for each sugar derivative, corresponding to the α- and β-forms of furanose and pyranose rings. In association with mass spectrometry analysis, each peak can be identified precisely, based on the profile of fragmentation observed. Fragmentation of TMS derivatives of hexoses usually generates diagnostic peaks at $m/z$ 217 and 214. Pyranose rings give rise to a ratio of $(m/z\ 204)/(m/z\ 217)$ of >1, whereas the ratio of furanose rings is <1. Peaks with retention times corresponding to standard derivatives of the typical cryptococcal GalXM components, mannose (Man), xylose (Xyl), galactose (Gal), and glucuronic acid (GlcA) were detected in the hydrolysates. For GalXM samples, Gal was the major monosaccharide constituent, followed by Man and Xyl. Proportions of monosaccharide constituents were similar in cap59
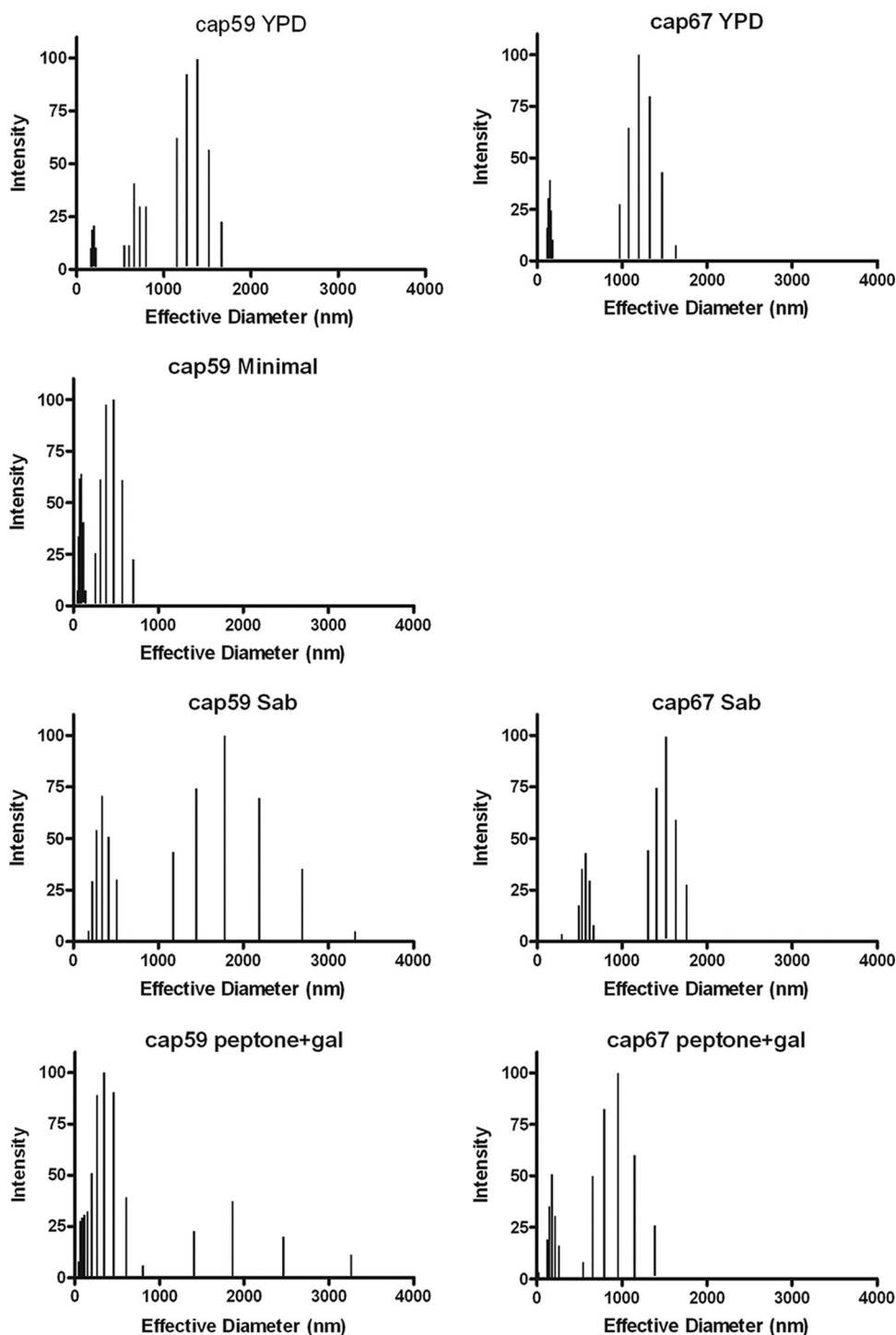
FIG. 2. Effective diameter and multimodal size distribution of GalXM from strains cap59 and cap67 grown in YPD medium, minimal medium, Sabouraud's dextrose broth (Sab), and peptone medium supplemented with 2% galactose. Effective diameter of GalXM from cap67 in minimal medium could not be determined due to poor polysaccharide yields. The *x* axis represents the diameter size distribution of the GalXM particles measured in nanometers. The *y* axis corresponds to the percent intensity of weighted sizes (14). Note that there is no panel for GalXM from cap67 grown in minimal medium because we were unable to recover sufficient polysaccharide for this type of analysis in those conditions.

and cap67 GalXMs, which presented Gal/Man/Xyl average molar ratios of 3.5:1.2:1 and 3.2:1.6:1, respectively (Table 1). GlcA was present in most of the GalXM samples derived from growing cultures at different temperatures, with an average molar ratio of 2.2%. Glucuronic acid was not present under all medium conditions tested. *N*-Acetyl galactosamine was the only sugar other than Man, Gal, and Xyl detected in the cap59, with a molar ratio of 3.6% (data not shown). The method used
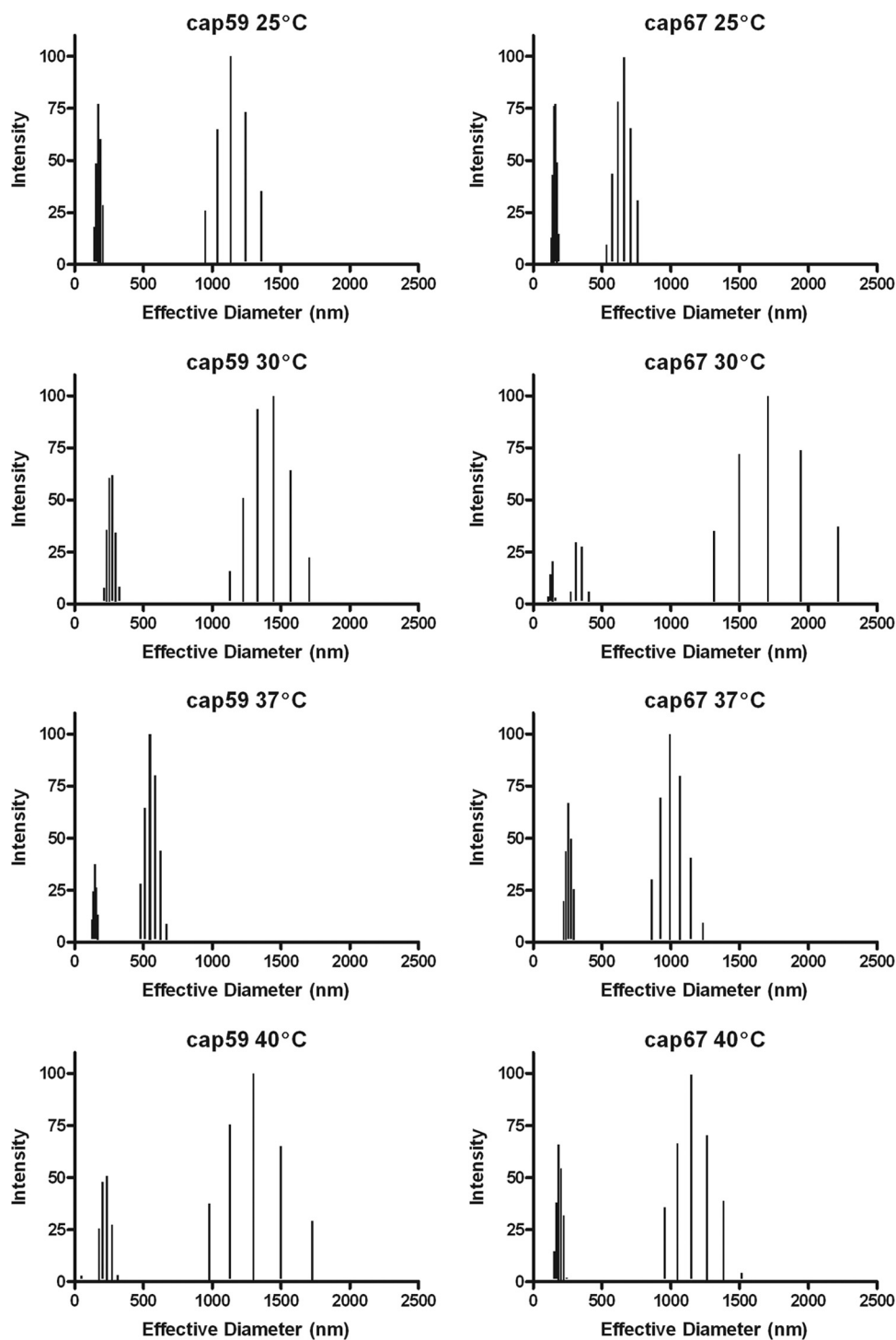
FIG. 3. Effective diameter and multimodal size distribution of GalXM from strains cap59 and cap67 grown in peptone supplemented with 2% galactose at 25°C, 30°C, 37°C, and 40°C. The *x* axis represents the diameter size distribution of the GalXM particles measured in nanometers. The *y* axis corresponds to the percent intensity of weighted sizes (14).

significantly underestimates glucuronic content, and these numbers should be considered in light of this fact.

**Average molecular mass, radius of gyration, and second virial coefficients of GalXM samples.** Multiangle laser light scattering was used to determine the average molecular mass

($M_w$) of GalXM from cap59 and cap67 acapsular mutants. The masses of the different GalXM preparations were calculated from Zimm plots (Table 2). The mass for GalXM for cap59 was about 8-fold greater than that for cap67 (Table 2). The radius of gyration (Rg) and the second virial coefficient ($A_2$)

TABLE 3. Effects of medium on GalXM size

| GalXM type and condition | | Effective diam (nm)[b] | Polydispersity[b] | Size distribution ranges (nm)[d] |
|---|---|---|---|---|
| Strain | Medium[a] | | | |
| cap59 | YPD | 783 ± 4 | 0.287 ± 0.011 | 150–200, 250–800, 1,100–1,670 |
| cap67 | YPD | 526 ± 14 | 0.429 ± 0.01 | 120–185, 975–1630 |
| cap59 | Minimal | 175 ± 4 | 0.413 ± 0.01 | 50–145, 260–710 |
| cap67 | Minimal | NA[c] | NA | NA |
| cap59 | Sab | 657 ± 36 | 0.362 ± 0.01 | 180–512, 1,173–3,315 |
| cap67 | Sab | 976 ± 12 | 0.203 ± 0.01 | 490–663, 1,300–1,762 |
| cap59 | Pep-Gal | 592 ± 13 | 0.338 ± 0.01 | 215–300, 1,130–1,710 |
| cap67 | Pep-Gal | 696 ± 58 | 0.373 ± 0.007 | 109–162, 273–400, 1,300–2,220 |

[a] Sab, Sabouraud's broth; Pep-Gal, peptone supplemented with galactose.
[b] Error was calculated from 10 measurements of one sample.
[c] NA, data not available.
[d] Predominant fragment sizes are given.

TABLE 4. Effects of temperature on GalXM size[a]

| GalXM type and condition | | Effective diam (nm)[b] | Polydispersity[b] | Size distribution ranges (nm)[c] |
|---|---|---|---|---|
| Strain | Temp (°C) | | | |
| cap59 | 25 | 378 ± 15 | 0.404 ± 0.01 | 144–206, 950–1,360 |
| cap67 | 25 | 280 ± 6 | 0.295 ± 0.004 | 130–186, 534–760 |
| cap59 | 30 | 592 ± 13 | 0.338 ± 0.01 | 215–300, 1,130–1,710 |
| cap67 | 30 | 696 ± 58 | 0.373 ± 0.007 | 109–162, 273–400, 1,300–2,220 |
| cap59 | 37 | 346 ± 7 | 0.254 ± 0.008 | 90–100, 207–260 |
| cap67 | 37 | 496 ± 10 | 0.284 ± 0.01 | 123–170, 585–880 |
| cap59 | 40 | 330 ± 15 | 0.359 ± 0.008 | 49, 178–272, 980–1,500 |
| cap67 | 40 | 435 ± 9 | 0.374 ± 0.008 | 150–240, 960–1,520 |

[a] Cells were grown in peptone supplemented with galactose.
[b] Error was calculated from 10 measurements of one sample.
[c] Predominant fragment sizes are given.

were also calculated from the light scattering data (Table 2). The Rg can be described as the average distance from the center point of PS to the outer edge of the molecule (average measure of the molecular size). The Rg for the different GalXM samples manifested significant differences, with 207 nm and 120 nm for cap59 and cap67, respectively. The Rg was used in conjunction with the $M_w$ to calculate the mass density of each GalXM sample. This analysis revealed that cap59 GalXM was 4-fold denser than the GalXM obtained from cap67 (Table 2). The second virial coefficient ($A_2$) is a property which describes the interaction strength between the molecule and a solvent, hence giving insights into the tendency of PS aggregation in that solvent. $A_2$ measurements for the different GalXM samples showed important differences. GalXM PS purified from the cap59 mutant was $0.26 \times 10^{-3} \pm 0.12 \times 10^{-3}$ cm$^3$ mol/g$^2$, suggesting higher molecule-solvent interaction strengths than PS isolated from cap67, which manifested a negative $A_2$ value ($-4.20 \times 10^{-3} \pm 3.6 \times 10^{-3}$ cm$^3$ mol/g$^2$), suggesting that molecule-solvent interaction strengths in cap67 are much lower than the molecule-molecule interaction strengths, resulting in a higher tendency for PS aggregation.

**Zeta potential, mobility, and frequency shift.** Zeta potential was determined for GalXM preparations from both cap67 and cap59 under different medium conditions and temperatures. For strain cap59 the zeta potentials were $-13.40 \pm 0.88$ mV (mean ± standard error of the mean [SEM]) in minimal medium, $-8.04 \pm 0.96$ mV in Sabouraud's broth, $-13.09 \pm 3.34$ mV in peptone supplemented with galactose, and $-7.67 \pm 0.26$ mV in YPD medium. For cap67 the zeta potential values were $-10.39 \pm 0.44$ mV in minimal medium, $-5.75 \pm 0.28$ mV in Sabouraud's broth, $-15.51$ mV in peptone supplemented with galactose, and $-5.97 \pm 0.85$ mV in YPD medium. These results suggest that the cryptococcal growth medium can affect the zeta potential of the GalXM produced (Fig. 1). When the glycosyl composition was analyzed, we found that the samples with the most negative zeta potential were most likely to test positive for glucuronic acid in the glycosyl analysis, consistent with the notion that such samples had higher content of this negatively charged constituent. We tested whether growth temperature could also alter the zeta potential of the GalXM produced. For GalXM from strain cap59, zeta potential mea-

surements were $-16.91 \pm 0.92$ at 25°C, $-13.09 \pm 3.34$ mV at 30°C, $-19.26 \pm 2.64$ at 37°C, and $-15.17 \pm 1.49$ mV at 40°C. For GalXM from strain cap67, zeta potential measurements were $-15.04 \pm 1.01$ at 25°C, $-11.43 \pm 1.23$ mV at 30°C, $-14.63 \pm 1.01$ at 37°C, and $-11.63 \pm 0.92$ mV at 40°C. These results suggest that growth temperature had as smaller effect on the GalXM zeta potentials than growth medium (Fig. 1).

**Effective diameter and multimodal size distribution analysis of GalXM.** To gain additional insight into the structural relationship between cap59 and cap67 GalXMs, we determined average effective diameters and size distributions of PS in different media and at different temperatures using multiangle light scattering. Although GalXM from both strains was comprised of populations of various diameters, it is clear that both the culture medium and growth temperature could affect the effective diameter and polydispersity of GalXM preparations. The effective diameter of GalXM from cap67 in minimal medium could not be determined since GalXM extractions under these conditions did not yield any polysaccharide. Polydispersity is a measure of the particle size distribution. We observed variation in GalXM effective diameters for both strains depending on growth medium conditions. This variation was most apparent for cap59 GalXM. We observed modest shifts in effective diameters as growth temperature was increased. The largest diameters were detected at 30°C for both cap59 and cap67 GalXM (Fig. 2 and 3 and Tables 3 and 4). The dynamic light-scattering parameters of cap59 and cap67 GalXMs derived from cultures grown in peptone and galactose at 30°C were measured as a function of salt concentration. The results revealed different responses for cap59 and cap67 GalXM as a function of salt concentration (Fig. 4 and Table 5).

**Antigenic differences between *C. neoformans* serotype A and D GalXMs.** A polyclonal serum against GalXM was obtained from mice immunized with a GalXM-*Bacillus anthracis* protective antigen (PA) conjugate (9, 10). The polyclonal antibody to GalXM was slightly reactive with cap59 GalXM and strongly reactive with cap67 GalXM by ELISA (data not shown). The immunofluorescence pattern of antibody binding to GalXM in encapsulated cryptococcal cells is dot- or punctate-like (10). When we compared different strains, we noted wide discrepancies in the number of dots surrounding individual cells and
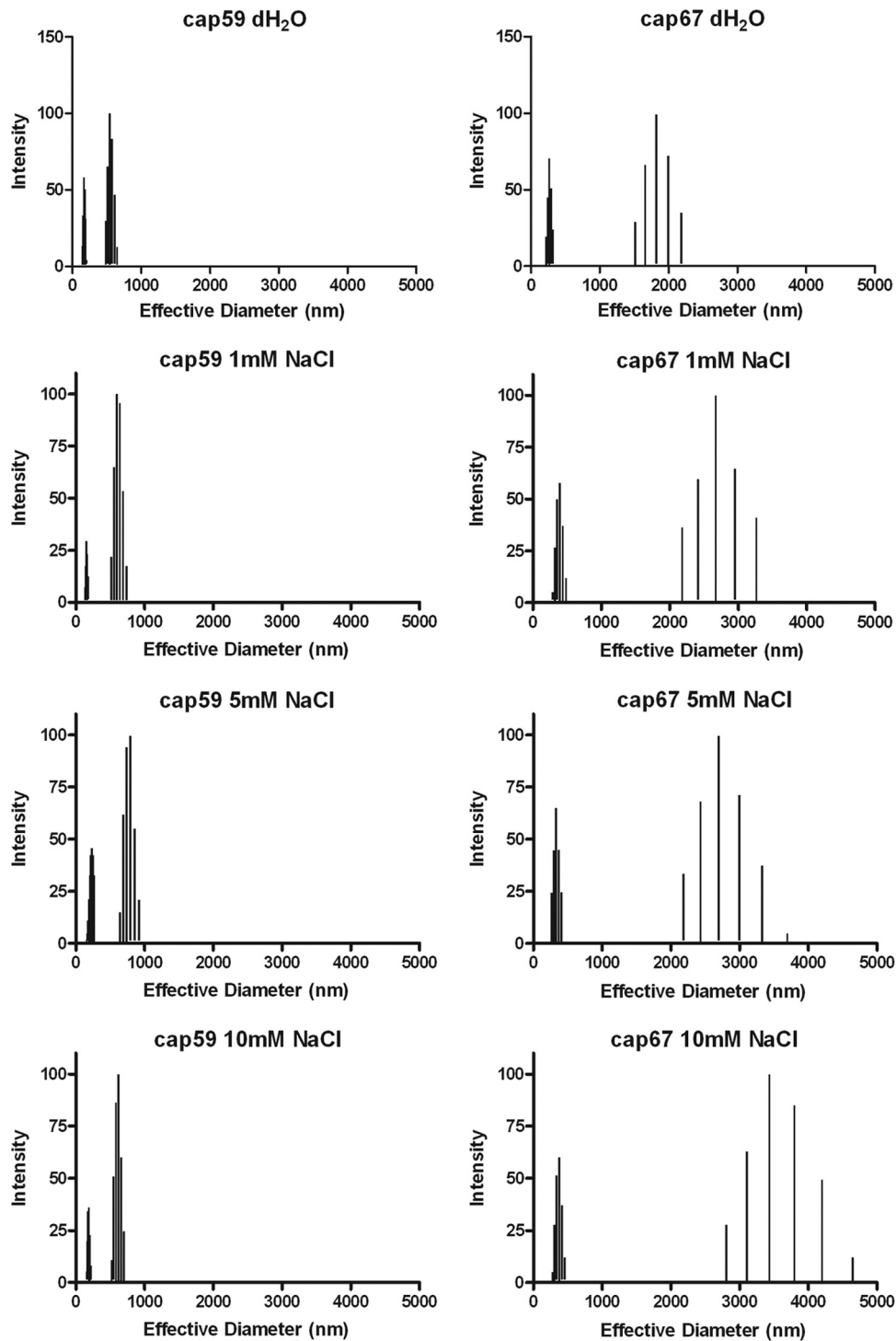
FIG. 4. Effective diameter and multimodal size distribution of GalXM from strains cap59 and cap67 grown in peptone supplemented with 2% galactose as a function of salt concentration. GalXM from each strain studied was diluted in distilled water (dH$_2$O) or 1 mM, 5 mM, and 10 mM NaCl. $x$ and $y$ axes are the same as in Fig. 1 and 2.

estimated the reactivity of the polyclonal antibody and/or amount of GalXM/cell by counting the average number of dots per cell. We tested eight strains each of serotype A and D and looked at the percentage of labeled cells. Using this measurement, we found that the percentages of labeling differed be-

tween A and D serotypes ($P < 0.01$) (Fig. 5). Seven strains of *C. gattii* (serotypes B and C) were also studied, and none stained with the polyclonal antibody to serotype D GalXM (data not shown).

To investigate the dynamics of GalXM production in *C.*

TABLE 5. Effects of NaCl on GalXM size[a]

| Diluent and GalXM source strain[b] | Effective diam (nm)[c] | Polydispersity[c] | Size distribution ranges (nm)[d] |
|---|---|---|---|
| dH$_2$0 | | | |
| cap59 | 319 ± 2 | 0.239 ± 0.008 | 151–203, 486–651 |
| cap67 | 630 ± 33 | 0.356 ± 0.008 | 220–319, 1,518–2,190 |
| 1 mM NaCl | | | |
| cap59 | 414 ± 5 | 0.262 ± 0.017 | 146–181, 521–740 |
| cap67 | 936 ± 69 | 0.373 ± 0.019 | 323–483, 2,186–3,268 |
| 5 mM NaCl | | | |
| cap59 | 409 ± 5 | 0.266 ± 0.006 | 182–269, 645–920 |
| cap67 | 834 ± 8 | 0.392 ± 0.011 | 269–409, 2,188–3,696 |
| 10 mM NaCl | | | |
| cap59 | 401 ± 4 | 0.291 ± 0.013 | 171–217, 523–702 |
| cap67 | 1081 ± 141 | 0.552 ± 0.142 | 277–459, 2,809–4,646 |

[a] Cells were grown in peptone supplemented with galactose.
[b] dH$_2$O, distilled water.
[c] Error was calculated from 10 measurements of one sample.
[d] Predominant fragment sizes are given.

*neoformans*, we studied antibody to GalXM binding as a function of growth time for strains B3501 (serotype D), 24067 (serotype D), and H99 (serotype A) in 12-h intervals for 2.5 days. The results revealed a sigmoidal pattern in GalXM staining as a function of time, which paralleled the shape of the *C. neoformans* growth curve except that it occurred 12 to 24 h later (Fig. 6). The highest percentage of GalXM staining was found in the stationary phase (Fig. 6A, B, and C). To further quantify GalXM production, we categorized the labeled cells into four groups depending on their number of fluorescence dots (Fig. 6D, E, and F). The results revealed a change in GalXM production with time. Toward the end of log phase at 24 h, the labeled *C. neoformans* showed a high percentage of the weakly labeled group, i.e., 1 to 5 dots per cell, indicating the low GalXM production during the active replication of the fungal population (Fig. 6D, E, and F). In contrast, in stationary phase, i.e., at >36 h, the labeled cell possessed a much stronger labeling pattern, as shown by the increasing number of fluorescence dots with time. Figure 7 shows representative examples of the cells counted in this assay. Despite these growth effects on GalXM expression, we note that the quantitative differences in staining described above were not a consequence of the kinetics of fungal growth since all studies used cells from 48-h or stationary-phase cell cultures.

## DISCUSSION

Earlier studies suggested that GalXM was structurally heterogeneous since its galactose, mannose, and xylose components could potentially be linked in 15 different ways (17). The biochemical complexity of that data suggested that the purified GalXM fractions could be part of a composite of several closely related antigens (17). Using proton NMR in an earlier study, we also found subtle differences among the different GalXM molecules (10). These data in turn implied that fine structural differences in the GalXM molecule could translate into antigenic variability (10). Here, we explore these differences using composition analysis, molecular

weight, zeta potential, polydispersity measurements, and immunofluorescence.

GalXM derived from the acapsular *C. neoformans* var. *neoformans* and *C. neoformans* var. *grubii* strains each contained galactose, mannose, and xylose but differed in the molar percentage of these components. Different media resulted in the production of GalXMs with different structural and physical properties, suggesting that studies of GalXM function should carefully control for nutritional conditions during culture growth. In contrast, the GalXM structure was more stable with respect to growth temperature. We also confirmed the presence of glucuronic acid in our GalXM preparations, as reported in a recent study (16). Since glucuronic acid is difficult to measure accurately relative to the other monosaccharide components, we used zeta potential measurements as a surrogate measure for the presence of negatively charged constituents in GalXM. Zeta potential measurements revealed a negative charge for all GalXM preparations from both cap67 and cap59 under different medium conditions. GalXM samples with the highest negative zeta potential were more likely to show the presence of glucuronic acid. These results, together with the prior report of glucuronic acid in GalXM, establish that this polysaccharide, like GXM, is negatively charged.

We explored the structural relationship between GalXM derived from cap59 (serotype A) and cap67 (serotype D). Static light-scattering measurements revealed that the average molecular mass of the GalXM from variety *C. neoformans* var. *grubii* was ~8-fold larger than that of *C. neoformans* var. *neoformans*. From the Rg and $M_w$ we calculated the mass density, and the results revealed that cap59 GalXM was 4-fold denser than the cap67 GalXM. These differences might also suggest differences in internal structure conformations (or shape factor) between both PS. Dynamic light scattering revealed that GalXM from both strains was comprised of a population of various diameters and that the relative distribution of diameters and extent of polydispersity were affected by both the growth medium and temperature. The ionic strength also affected the measured polydispersity, suggesting that GalXM conformational variability is a function of anion and cation concentration. In this regard, the effective diameters in cap59
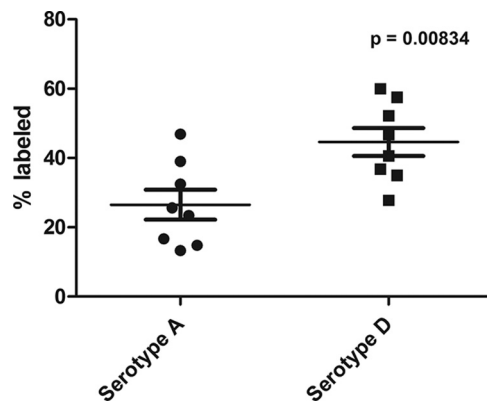


FIG. 5. Percentage of cells labeled by polyclonal antibody to GalXM among eight strains of serotypes A and D after 48 h of culture growth. Serotype D strains show a higher percentage of labeled cells than serotype A strains ($P < 0.01$).
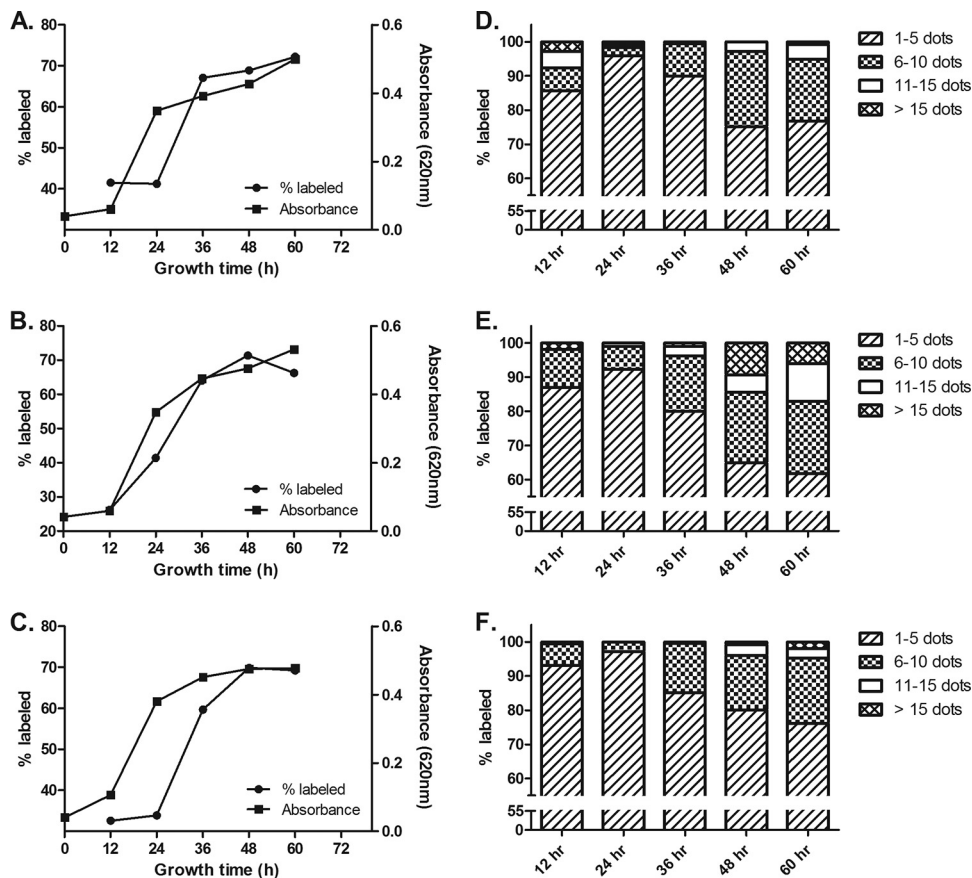
FIG. 6. GalXM immunofluorescence staining was dependent on growth phase in *C. neoformans*. Strains B3501 (serotype D) (A), 24067 (serotype D) (B), and H99 (serotype A) (C) each showed comparable patterns in both growth kinetics and GalXM labeling as a function of culture time. Maximum GalXM staining occurred in the stationary phase. Panels D, E, and F show the frequency of dots per cell and as a function of time for strains B3501, 24067, and H99, respectively. Fig. 7 shows representative examples of the cells counted in this assay.

become smaller as salt concentration is increased while in cap67 the effective diameters increased. This difference in response may reflect differences in charge positioning in the GalXMs of these strains, which in turn would imply differences in primary structural arrangements of the monosaccharide constituents.

We note that the mass of the cap67 GalXM reported here is larger than that reported in our prior study (21). Given all the structural variability uncovered by the current study, we attribute that difference to the culture growth conditions used to prepare GalXM in the prior and current study. In the earlier study cap67 cultures were grown in Sabouraud's dextrose broth; in this study we used peptone supplemented with 2% galactose since we found that this medium gave a higher yield of purified GalXM. Lastly, we note differences in the sign of the second virial coefficient value for GalXMs from cap59 and cap67 measured by static light scattering. Positive and negative values for the second virial coefficient reflect globally repulsive and attractive intermolecular interactions, respectively, providing an additional parameter for differences between the GalXMs produced by these strains.

In considering the biological implications of these results, it is important to note one potential limitation of the work described here, namely, reliance on GalXM derived from acap-

sular strains. This reliance on using GalXM from acapsular strains is necessitated by the fact that there are currently no methodologies that completely separate GalXM from GXM, especially given data that these two polysaccharides can interact (12). Since culture supernatants from encapsulated strains contain copious amounts of GXM, all structural studies of GalXM have relied on material from acapsular strains. However, this introduces a potential systematic problem for GalXM studies because the phenotype of acapsular strains like cap67 and cap59 may reflect a secretion defect (15). Hence, it is conceivable that the GalXM from acapsular strains has structural differences from that of wild-type strains. Currently, there is no methodology to ascertain whether this concern is real since attempts to develop better serological reagents in the form of monoclonal antibodies (MAbs) have not proved successful, and we lack reagents to compare the GalXM structures in capsular and their acapsular mutants (10).

Given the potential limitations inherent in working with acapsular strains noted above and the paucity of well-characterized acapsular mutants expressing the same genetic defect such as strains cap67 and cap59, we investigated GalXM variability in wild-type strains by evaluating their reactivity for immune serum reactive with GalXM. All serotype A and D strains reacted with immune serum generated against GalXM
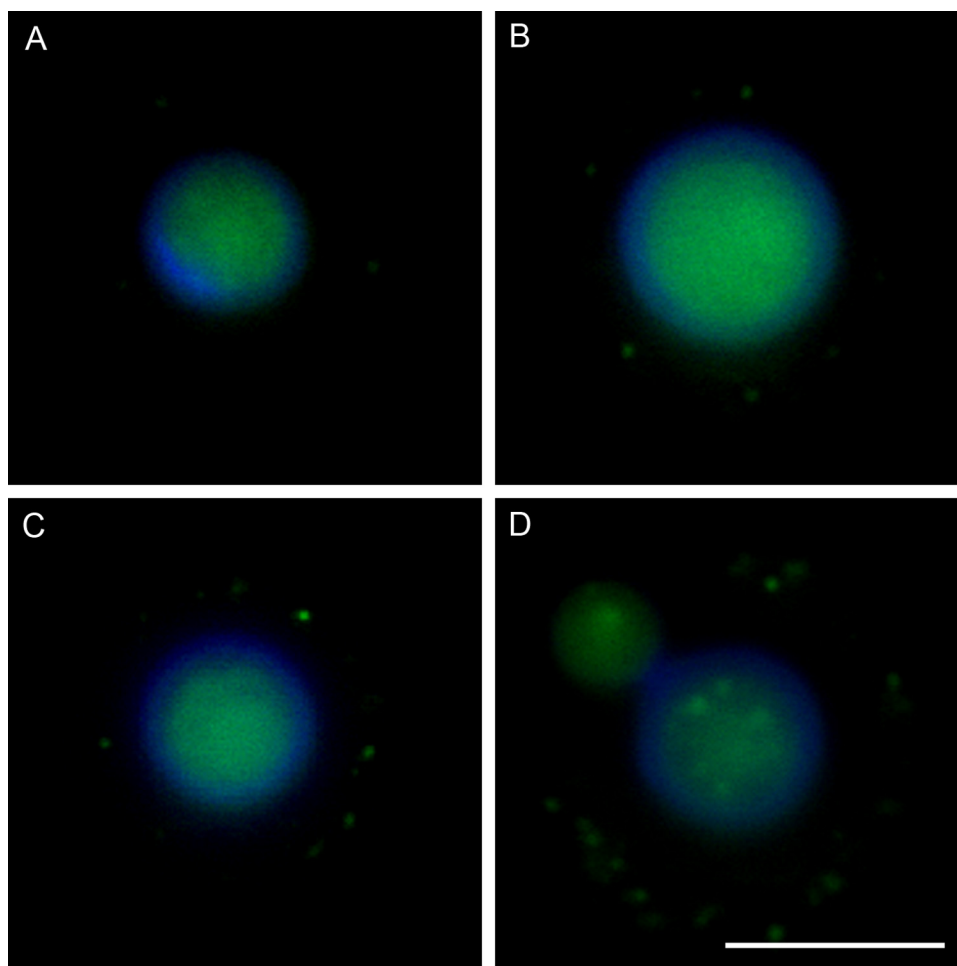
FIG. 7. Four representative images of GalXM antibody staining. Cells are labeled differently according to the amount of GalXM in the capsule. The labeling intensities are categorized into four groups: 1 to 5 (A), 6 to 10 (B), 11 to 15 (C), and >15 dots (D). The blue rim around the cell body is the result of calcofluor staining. The green fluorescence in the cell body may reflect autofluorescence and/or antibody to GalXM binding to cell wall as reported for acapsular cells (10) Scale bar, 5 μm.

from serotype D, with serotype D strains producing stronger reactivity. Serum reactivity with cryptococcal cells was a function of growth phase for both serotype A and D strains, and was most prominent in stationary-phase cells. In contrast, no immunoreactivity was observed with any of the *C. gattii* strains. We interpret these results as indicating that GalXMs from serotypes A and D share antigenic determinants that presumably reflect the presence of common structural motifs not found in *C. gattii* strains. Hence, the serological studies imply quantitative differences in GalXM epitope content between A and D strains that could reflect differences in GalXM amount and/or chemical structure.

In summary, we report large intra- and interstrain variability in the structure, serological reactivity, and physical properties of GalXM as a function of growth conditions. One practical consequence of these results is that experiments comparing GalXM structural properties must take into account growth conditions. Given this structural variability, it is possible that GalXM made *in vivo* is structurally different from that made in culture. In fact, it is conceivable that interstrain and growth-related differences in GalXM structure are responsible for

discrepant results observed regarding serological cross-reactivity of the polysaccharide with other antigens (7, 8). Given that GalXM has now been associated with profound immunological derangements (26, 27, 30), it is likely that this polysaccharide makes a contribution to the virulence composition of *C. neoformans* (9, 20, 23). Since the biological properties of GalXM must reflect its structure, we suspect that structural variability could translate into variable effects in host damaging effects.

## REFERENCES

1. **Bose, I., A. J. Reese, J. J. Ory, G. Janbon, and T. L. Doering.** 2003. A yeast under cover: the capsule of *Cryptococcus neoformans*. Eukaryot. Cell **2:**655–663.

2. **Chaka, W., A. F. Verheul, V. V. Vaishnav, R. Cherniak, J. Scharringa, J. Verhoef, H. Snippe, and I. M. Hoepelman.** 1997. *Cryptococcus neoformans* and cryptococcal glucuronoxylomannan, galactoxylomannan, and mannoprotein induce different levels of tumor necrosis factor alpha in human peripheral blood mononuclear cells. Infect. Immun. **65:**272–278.

3. **Chang, Y. C., and K. J. Kwon-Chung.** 1994. Complementation of a capsule-deficient mutation of *Cryptococcus neoformans* restores its virulence. Mol. Cell. Biol. **14:**4912–4919.

4. **Chaskes, S., S. Frases, M. Cammer, G. Gerfen, and A. Casadevall.** 2008. Growth and pigment production on D-tryptophan medium by *Cryptococcus gattii*, *Cryptococcus neoformans*, and *Candida albicans*. J. Clin. Microbiol. **46:**255–264.

5. **Cherniak, R., R. Reiss, and S. H. Turner.** 1982. A galactoxylomannan antigen of *Cryptococcus neoformans* serotype A. Carbohydr. Res. **103:**239–250.

6. **Cherniak, R., and J. B. Sundstrom.** 1994. Polysaccharide antigens of the capsule of *Cryptococcus neoformans*. Infect. Immun. **62:**1507–1512.

7. **Dalle, F., P. E. Charles, K. Blanc, D. Caillot, P. Chavanet, F. Dromer, and A. Bonnin.** 2005. *Cryptococcus neoformans* Galactoxylomannan contains an epitope (s) that is cross-reactive with *Aspergillus* galactomannan. J. Clin. Microbiol. **43:**2929–2931.

8. **De Jesus, M., E. Hackett, M. Durkin, P. Connolly, A. Casadevall, R. Petraitiene, T. J. Walsh, and L. J. Wheat.** 2007. Galactoxylomannan does not exhibit cross-reactivity in the platelia *Aspergillus* enzyme immunoassay. Clin. Vaccine Immunol. **14:**624–627.

9. **De Jesus, M., A. M. Nicola, S. Frases, I. R. Lee, S. Mieses, and A. Casadevall.** 2009. Galactoxylomannan-mediated immunological paralysis results from specific B cell depletion in the context of widespread immune system damage. J. Immunol. **183:**3885–3894.

10. **De Jesus, M., A. M. Nicola, M. L. Rodrigues, G. Janbon, and A. Casadevall.** 2009. Capsular localization of the *Cryptococcus neoformans* polysaccharide component galactoxylomannan. Eukaryot. Cell **8:**96–103.

11. **Dubois, M., K. A. Gilles, J. K. Hamilton, P. A. Rebers, and F. Smith.** 1956. Colorimetric method for determination of sugars and related substances. Anal. Chem. **28:**350–356.

12. **Frases, S., L. Nimrichter, N. B. Viana, A. Nakouzi, and A. Casadevall.** 2008. *Cryptococcus neoformans* capsular polysaccharide and exopolysaccharide fractions manifest physical, chemical, and antigenic differences. Eukaryot. Cell **7:**319–327.

13. **Frases, S., B. Pontes, L. Nimrichter, N. B. Viana, M. L. Rodrigues, and A. Casadevall.** 2009. Capsule of *Cryptococcus neoformans* grows by enlargement of polysaccharide molecules. Proc. Natl. Acad. Sci. U. S. A. **106:**1228–1233.

14. **Frases, S., A. Salazar, E. Dadachova, and A. Casadevall.** 2007. *Cryptococcus neoformans* can utilize the bacterial melanin precursor homogentisic acid for fungal melanogenesis. Appl. Environ. Microbiol. **73:**615–621.

15. **Garcia-Rivera, J., Y. C. Chang, K. J. Kwon-Chung, and A. Casadevall.** 2004. *Cryptococcus neoformans* CAP59 (or Cap59p) is involved in the extracellular trafficking of capsular glucuronoxylomannan. Eukaryot. Cell **3:**385–392.

16. **Heiss, C., J. S. Klutts, Z. Wang, T. L. Doering, and P. Azadi.** 2009. The structure of *Cryptococcus neoformans* galactoxylomannan contains beta-D-glucuronic acid. Carbohydr Res. **344:**915–920.

17. **James, P. G., and R. Cherniak.** 1992. Galactoxylomannans of *Cryptococcus neoformans*. Infect. Immun. **60:**1084–1088.

18. **James, P. G., R. Cherniak, R. G. Jones, C. A. Stortz, and E. Reiss.** 1990. Cell-wall glucans of *Cryptococcus neoformans* Cap 67. Carbohydr. Res. **198:**23–38.

19. **Levitz, S. M., and C. A. Specht.** 2006. The molecular basis for the immunogenicity of *Cryptococcus neoformans* mannoproteins. FEMS Yeast Res. **6:**513–524.

20. **McClelland, E. E., P. Bernhardt, and A. Casadevall.** 2006. Estimating the relative contributions of virulence factors for pathogenic microbes. Infect. Immun. **74:**1500–1504.

21. **McFadden, D. C., M. De Jesus, and A. Casadevall.** 2006. The physical properties of the capsular polysaccharides from *Cryptococcus neoformans* suggest features for capsule construction. J. Biol. Chem. **281:**1868–1875.

22. **Mitchell, T. G., and J. R. Perfect.** 1995. Cryptococcosis in the era of AIDS—100 years after the discovery of *Cryptococcus neoformans*. Clin. Microbiol. Rev. **8:**515–548.

23. **Moyrand, F., T. Fontaine, and G. Janbon.** 2007. Systematic capsule gene disruption reveals the central role of galactose metabolism on *Cryptococcus neoformans* virulence. Mol. Microbiol. **64:**771–781.

24. **Mukherjee, J., A. Casadevall, and M. D. Scharff.** 1993. Molecular characterization of the humoral responses to *Cryptococcus neoformans* infection and glucuronoxylomannan-tetanus toxoid conjugate immunization. J. Exp. Med. **177:**1105–1116.

25. **Perfect, J. R., and A. Casadevall.** 2002. Cryptococcosis. Infect. Dis. Clin. North Am. **16:**837–874, v–vi.

26. **Pericolini, E., E. Cenci, C. Monari, M. De Jesus, F. Bistoni, A. Casadevall, and A. Vecchiarelli.** 2006. *Cryptococcus neoformans* capsular polysaccharide component galactoxylomannan induces apoptosis of human T-cells through activation of caspase-8. Cell. Microbiol. **8:**267–275.

27. **Pericolini, E., E. Gabrielli, E. Cenci, M. De Jesus, F. Bistoni, A. Casadevall, and A. Vecchiarelli.** 2009. Involvement of glycoreceptors in galactoxylomannan-induced T cell death. J. Immunol. **182:**6003–6010.

28. **Steenbergen, J. N., and A. Casadevall.** 2000. Prevalence of *Cryptococcus neoformans* var. *neoformans* (serotype D) and *Cryptococcus neoformans* var. *grubii* (serotype A) isolates in New York City. J. Clin. Microbiol. **38:**1974–1976.

29. **Vaishnav, V. V., B. E. Bacon, M. O'Neill, and R. Cherniak.** 1998. Structural characterization of the galactoxylomannan of *Cryptococcus neoformans* Cap67. Carbohydr. Res. **306:**315–330.

30. **Villena, S. N., R. O. Pinheiro, C. S. Pinheiro, M. P. Nunes, C. M. Takiya, G. A. DosReis, J. O. Previato, L. Mendonca-Previato, and C. G. Freire-de-Lima.** 2008. Capsular polysaccharides galactoxylomannan and glucuronoxylomannan from *Cryptococcus neoformans* induce macrophage apoptosis mediated by Fas ligand. Cell. Microbiol. **10:**1274–1285.

31. **Zaragoza, O., M. L. Rodrigues, M. De Jesus, S. Frases, E. Dadachova, and A. Casadevall.** 2009. The capsule of the fungal pathogen *Cryptococcus neoformans*. Adv. Appl. Microbiol. **68:**133–216.